Numerical Analysis of the Piston Secondary Dynamics in Reciprocating Compressors

Tae-Jong Kim*

School of Mechanical Engineering and Research Institute of Mechanical Technology,
Pusan National University, Pusan 609-735, Korea

In this study, a numerical analysis for the piston secondary dynamics of small refrigeration reciprocating compressors is performed. In general, the length of cylinder in this class of compressors is shortened to diminish the frictional losses of the piston-cylinder system. So, the contacting length between piston and cylinder wall is in variable with the rotating crank angle around the BDC of the reciprocating piston. In the problem formulation of the piston dynamics, the variation in bearing length of the piston and all corresponding forces and moments are considered in order to determine the piston trajectory, velocity and acceleration at each step. A Newton-Raphson procedure was employed in solving the secondary dynamic equations of the piston. The developed computer program can be used to calculate the entire piston trajectory and the lubrication characteristics as functions of crank angle under compressor running conditions. The results explored the effects of some design parameters and operating conditions on the stability of the piston, the oil leakage, and friction losses.

Key Words : Reciprocating Compressors, Piston Secondary Dynamics, Hydrodynamic Lubrication, Piston Trajectory, Oil leakage, Friction Loss

1. Introduction

Piston-cylinder systems are widely used in power engineering applications. In a reciprocating compressor used in domestic refrigerators, where extremely low friction loss is required, ringless pistons are being used to eliminate the friction between piston and cylinder wall. And, the length of cylinder bore is decreased to diminish the frictional losses of the piston-cylinder system. Since the ringless piston has the freedom of lateral motion there is a potential danger that it will occasionally hit the cylinder while moving up and down along it's axis. A good design must therefore provide a smooth and stable reciprocating

E-mail : tjong@pusan.ac.kr
TEL : +82-51-510-2474; FAX : +82-51-514-7640
School of Mechanical Engineering and Research Institute of Mechanical Technology, Pusan National University, Pusan 609-735, Korea. (Manuscript Received June 8, 2002; Revised December 26, 2002)

motion of the piston and ensure that the oil film separating the piston from the cylinder wall is maintained all times. And, the compromise between the friction loss and refrigerant gas leakage through the piston-cylinder clearance is required utilizing a dynamic analysis of the secondary motion for the high efficiency compressor. As a calculation model of the piston secondary motion simulation, there are 2 models defining the piston impact of the cylinder wall. The first method calculates the thrust force of the piston in radial direction by solving the time dependent Reynolds equation for the lubricating fluid film. Early studies on this model by Li et al. (1983) and Zhu et al. (1992 ; 1993) solved the problem for reciprocating pistons in automotive engines. Gommed and Etsion in a series of papers (1993 ; 1994 ; 1995) considered gas lubrication of a ringless piston in a low heat rejection (LHR) engine. Parata et al. (2000) performed a dynamic analysis for the oil film between piston and cylinder in small refrigerating compressors. The other meth-

od calculates the piston impact forces by utilizing the equivalent mass, damping and stiffness of the cylinder wall at the contact points. (1997 ; 2000) The piston oscillatory motion in the cylinder bore is directly related to the lubrication characteristics of the piston–cylinder clearance. It is certainly necessary to develop and improve piston–cylinder lubrication analysis for better understanding of piston dynamics and reliable prediction of friction characteristics. In this paper, a problem formulation for the piston dynamics is presented considering the variation in bearing length of the piston and hydrodynamic forces and moments between piston and cylinder wall. The developed computer program can be used to calculate the entire piston trajectory, and the hydrodynamic lubrication characteristics as functions of crank angle under compressor running conditions. And the results explored the effects of the radial clearance, lubricant viscosity, length of the cylinder wall, and pin location on the stability of the piston, the oil leakage, and friction losses.

2. Piston Secondary Dynamics

2.1 Equations of motion

A piston-cylinder system in the reciprocating compressors is shown in Fig. 1 and the equations describing the piston secondary dynamics can be written in dimensionless form as,

$$T_x + F_h = m_p \ddot{x}_0 \tag{1}$$

$$M_f + M_h = I_p \ddot{a} \tag{2}$$

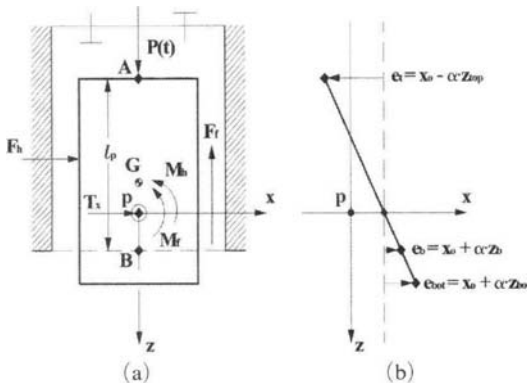**Fig. 1** FBD of the reciprocating piston

$$m_p = \frac{\omega C^3}{\mu R^4} \, \bar{m}_p, \; x_0 = \frac{\bar{x}_0}{C}, \; a = \frac{R}{C} \, \bar{a}, \; I_p = \frac{\omega}{\mu R^3} \left(\frac{C}{R} \right)^3 \bar{I}_p,$$

$$T_x = -\frac{1}{\mu \omega R^2} \left(\frac{C}{R} \right)^2 \bar{T}_x, \; F_h = \frac{1}{\mu \omega R^2} \left(\frac{C}{R} \right)^2 \bar{F}_h,$$

$$M_h = \frac{1}{\mu \omega R^3} \left(\frac{C}{R} \right)^2 \bar{M}_h, \; M_f = \frac{1}{\mu \omega R^3} \left(\frac{C}{R} \right)^2 \bar{M}_f$$

And, T_x is the radial component of the connecting rod force, F_h is the hydrodynamic force due to the pressure in the oil film. M_h and M_f are, respectively, the moments about the wrist-pin due to the F_h and F_f. The acceleration of piston center of mass in the x direction is $\ddot{x}_0$ and the angular acceleration is $\ddot{a}$. The boundary position B of the piston is not in fixed if the sum of piston length and stroke exceeds the length of the cylinder wall. The nondimensional accelerations $\ddot{x}_0$, $\ddot{a}$ can be found from the lateral accelerations $\ddot{\varepsilon}_t$, $\ddot{\varepsilon}_b$ of the two ends A, B of the reciprocating piston.

$$\ddot{x}_0 = \ddot{\varepsilon}_b - \left(\frac{\ddot{\varepsilon}_b - \ddot{\varepsilon}_t}{l_p} \right) z_b, \; \ddot{a} = (\ddot{\varepsilon}_b - \ddot{\varepsilon}_t)/l_p$$

$$l_p = \frac{\bar{l}_p}{R}, \; z_b = \frac{\bar{z}_b}{R}, \; \varepsilon_b = \frac{e_b}{C}, \; \varepsilon_t = \frac{e_t}{C} \tag{3}$$

Therefore, a substitution of the above equations into (1), (2) yields the governing equations of motion in the matrix form,

$$\begin{bmatrix} m_p \left(1 - \dfrac{z_b}{l_p} \right) & m_p \dfrac{z_b}{l_p} \\ \dfrac{I_p}{l_p} & -\dfrac{I_p}{l_p} \end{bmatrix} \begin{bmatrix} \ddot{\varepsilon}_b \\ \ddot{\varepsilon}_t \end{bmatrix} = \begin{bmatrix} T_x + F_h \\ M_f + M_h \end{bmatrix} \tag{4}$$

Equation (4) can be transformed to the following nonlinear equation system for the application of Newton–Raphson method.

$$f_1(\dot{\varepsilon}_b, \dot{\varepsilon}_t) = T_x + F_h - m_p \left[\ddot{\varepsilon}_b - (\ddot{\varepsilon}_b - \ddot{\varepsilon}_t) \frac{z_b}{l_p} \right] = 0 \tag{5}$$

$$f_2(\dot{\varepsilon}_b, \dot{\varepsilon}_t) = M_f + M_h - I_p(\ddot{\varepsilon}_b - \ddot{\varepsilon}_t)/l_p = 0 \tag{6}$$

2.2 Hydrodynamic analysis

The force and moment acting on the piston skirt, F_h and M_h, are due to the hydrodynamic pressure developed in the oil film, can be obtained from the Reynolds equation. The Reynolds equation for incompressible and laminar flow can be written in nondimensional form as

$$\frac{\partial}{\partial \theta}\left(h^3 \frac{\partial p}{\partial \theta}\right)+\frac{\partial}{\partial z}\left(h^3 \frac{\partial p}{\partial z}\right)=6 V_p \frac{\partial h}{\partial z}+12 \frac{\partial h}{\partial t} \quad (7)$$

$$h=1-(x_0+a \cdot z_i) \cos \theta \quad (8)$$

$$h=\frac{\bar{h}}{C}, \ t=\omega \bar{t}, \ z=\frac{\bar{z}}{R}, \ p=\frac{\bar{p}}{\mu \omega}\left(\frac{C}{R}\right)^2, \ V_p=\frac{\bar{V}_p}{\omega R}$$

where z_i is the axial distance from the origin p of the xz coordinates to the grid point of the bearing surface of the piston, h is the local oil film thickness for an eccentric and tilted piston, and V_p represents the piston axial velocity. This equation can be discretized with the conventional finite difference scheme. The hydrodynamic pressure can be expressed by using SOR (Successive Over Relaxation) method with over-relaxation parameter ω_c

$$p_{i,j}^{k+1}=p_{i,j}^k-\omega_c \frac{R_{i,j}}{B_{i,j}} \quad (9)$$

$$R_{i,j}=(A_{i,j}P_{i-1,j}^{k+1}+B_{i,j}P_{i,j}^k+C_{i,j}p_{i+1,j}^k \\ +D_{i,j}p_{i,j-1}^{k+1}+E_{i,j}p_{i,j+}^k)-F_{i,j}^k \quad (10)$$

$$A_{i,j}=\frac{h_{i-\frac{1}{2},j}^3}{(\Delta\theta)^2}, \ B_{i,j}=-\left[\frac{h_{i-\frac{1}{2},j}^3+h_{i+\frac{1}{2},j}^3}{(\Delta\theta)^2}+\frac{h_{i,j-\frac{1}{2}}^3+h_{i,j+\frac{1}{2}}^3}{(\Delta z)^2}\right],$$

$$C_{i,j}=\frac{h_{i+\frac{1}{2},j}^3}{(\Delta\theta)^2}, \ D_{i,j}=\frac{h_{i,j-\frac{1}{2}}^3}{(\Delta z)^2}, \ E_{i,j}=\frac{h_{i,j+\frac{1}{2}}^3}{(\Delta z)^2}$$

$$F_{i,j}=6 V_p\left(\frac{h_{i,j+\frac{1}{2}}-h_{i,j-\frac{1}{2}}}{\Delta z}\right)-12(\dot{x}_0+\dot{a}z_{i,j}) \cos \theta_{i,j}$$

The pressure in the oil film is known, both F_h and M_h can be determined as, respectively,

$$F_h=-\int_0^{2\pi}\int_0^{l_p} p(\theta, z) \cos \theta \ dz \cdot d\theta \quad (11)$$

$$M_h=-\int_0^{2\pi}\int_0^{l_p} [p(\theta, z) \cos \theta] z dz \cdot d\theta \quad (12)$$

And, the nondimensional viscous frictional force and moment can be obtained according to

$$F_f=-\frac{C}{R}\int_0^{2\pi}\int_0^{l_p}\left(\frac{h}{2}\frac{\partial p}{\partial z}+\frac{V_p}{h}\right) dz d\theta \quad (13)$$

$$M_f=\frac{C}{R}\int_0^{2\pi}\int_0^{l_p}\left(\frac{h}{2}\frac{\partial p}{\partial z}+\frac{V_p}{h}\right) \cos \theta \ dz d\theta \quad (14)$$

In integrating above Eqs., whenever cavitation occurred, the oil pressure was replaced by a gas pressure interpolated between dynamic cylinder pressure P_{cyl} and static suction pressure P_{sus}, depending on the cavitation axial location. Therefore, cyclically averaged power consumption can

be written in nondimensional form,

$$W_{avg}=\frac{1}{2\pi}\int_0^{2\pi}F_f \cdot V_p d\theta \quad (15)$$

The instantaneous volumetric oil leakage in nondimensional form throughout the clearance between piston and cylinder is given by

$$Q_z=\int_0^{2\pi}\left(\frac{V_p h}{2}-\frac{h^3}{12}\frac{\partial p}{\partial z}\right)\bigg|_{z=l_p} d\theta \quad (16)$$

2.3 Numerical procedure

The dynamic load capacity of fluid film between piston and cylinder confined in eccentricity, velocity, and acceleration of piston center is calculated under transient conditions. Instead of integrating the second-order governing equations of motion for the piston, Eq. (4), a Newton-Raphson method can be applied to the nonlinear system Eqs. (5) and (6). Assume that the initial values of $\varepsilon_b(t)$, $\varepsilon_t(t)$, $\dot{\varepsilon}_p(t)$, and $\dot{\varepsilon}_t(t)$ for the time step t. For the computational level i of the time step t, the previous values $\varepsilon_b(t)$, $\varepsilon_t(t)$, $\dot{\varepsilon}_b(t)$, $\dot{\varepsilon}_t(t)$ can be used for the initial of internal loop of the Newton-Rapson scheme. Then, lubricant film thickness $h(\theta, z, t)$, hydrodynamic pressure $p(\theta, z, t)$, and all the forces of moments of Eq. (4) including F_h, F_f, M_h are calculated. The adjustment of $\dot{\varepsilon}_b(t+\Delta t)$ and $\dot{\varepsilon}_t(t+\Delta t)$ can be done with a Newton-Raphson iterative scheme. From the solution of $\dot{\varepsilon}_b(t)$ and $\dot{\varepsilon}_t(t)$ at previous time step and the present values of $\dot{\varepsilon}_b(t+\Delta t)$ and $\dot{\varepsilon}_t(t+\Delta t)$ for the current time step, the accelerations can be computed by the numerical differentiation, $\ddot{\varepsilon}_b^i(t)=\frac{\dot{\varepsilon}_b(t+\Delta t)-\dot{\varepsilon}_b(t)}{\Delta t}$, $\ddot{\varepsilon}_t^i(t)=\frac{\dot{\varepsilon}_t(t+\Delta t)-\dot{\varepsilon}_t(t)}{\Delta t}$. For the next inner loop level $i+1$, $\ddot{\varepsilon}_b^{i+1}(t)$ and $\ddot{\varepsilon}_t^{i+1}(t)$ are calculated by using the newly adjusted solution of $\dot{\varepsilon}_b(t+\Delta t)$ and $\dot{\varepsilon}_t(t+\Delta t)$ in Newton-Raphson method. Once this is done, convergence criterion $\left|\frac{\dot{\varepsilon}_b^{i+1}-\dot{\varepsilon}_b^i}{\dot{\varepsilon}_b^{i+1}}\right|$, $\left|\frac{\dot{\varepsilon}_t^{i+1}-\dot{\varepsilon}_t^i}{\dot{\varepsilon}_t^{i+1}}\right| \leq 10^{-7}$ can be checked for satisfied or not. If it is not satisfied, the present solutions $\dot{\varepsilon}_b(t)$ and $\dot{\varepsilon}_t(t)$ for the current level will be adjusted and the above procedure can be repeated. Once the satisfactory $\dot{\varepsilon}_b(t)$, $\dot{\varepsilon}_t(t)$ are

Table 1　Design parameters of the reciprocation compressors and baseline values used in the simulation

Mass of the piston ($\bar{m}_p$)	0.043 kg
Moment of inertia of the piston ($\bar{I}_p$)	3.93×10^{-6} N·m·s^2
Radius of the piston (R)	11.5 mm
Length of the piston (L)	22 mm
Length of the cylinder (CYL)	28.85 mm
Rotating radius between crankshaft center and crank-pin center (R_o)	7.5 mm
Radial clearance between the piston and the cylinder wall (C)	4 μm
Lubricant viscosity (μ)	5 mPa·s

obtained, the piston position at the end of the current step can be determined by $\varepsilon_b(t+\Delta t) = \varepsilon_b(t) + \dot{\varepsilon}_b(t)\Delta t$, $\varepsilon_t(t+\Delta t) = \varepsilon_t(t) + \dot{\varepsilon}_t(t)\Delta t$. And then proceed to the next time step utilizing the solution $\dot{\varepsilon}_b(t+\Delta t)$, $\dot{\varepsilon}_t(t+\Delta t)$ of previous time step as the initial value of next step.

3. Results and Discussion

A computer program has been constructed based on the hydrodynamic lubrication model and Newton-Raphson scheme to solve the transient problem at each time step was converged successfully. From the numerical results, the influence of radial clearance, oil viscosity, pin location and length of cylinder wall on the piston dynamics, lubrication characteristics are examined. The results were obtained for a typical reciprocating compressor, and design parameters for the simulation is listed in Table 1. From Fig. 2, it can be shown that the force T_x acting on the piston from the dynamic analysis [10] of the compression mechanism is dynamically balanced by the hydrodynamic reaction force F_h along the radial direction. Similar results can be observed from Fig. 3 for the viscous frictional moment M_f and the hydrodynamic moment M_h about the piston-pin due to F_f and F_h. Results for the x-direction orbits of the piston center located at the piston top, piston-pin, piston boundary location, and piston bottom are shown in Fig. 4. This figure shows the converged periodic solution for the piston trajectory inside the cylinder within about 20~30 cycles depending on the values of design parameters. It can be shown that there are
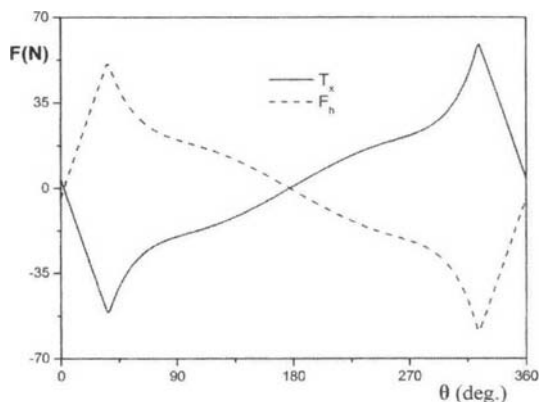
Fig. 2　Applied force T_x and oil film reaction force F_h versus crank angle θ of one revolution
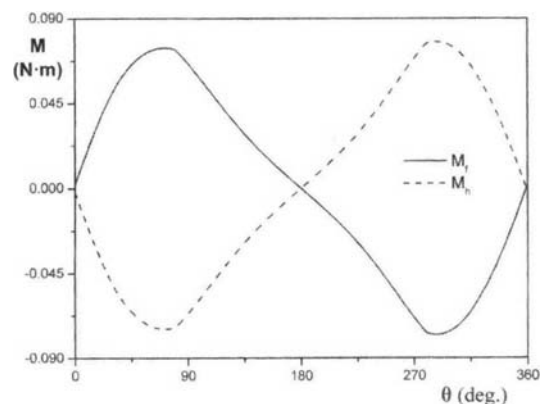
Fig. 3　Frictional moment M_f and oil film reaction moment M_h about the piston pin versus crank angle θ of one revolution

different trajectories between the boundary and bottom locations during the crank angle of 80.9°~278.8°. Due to the shortened length of the cylinder, the piston protrudes from the inside of
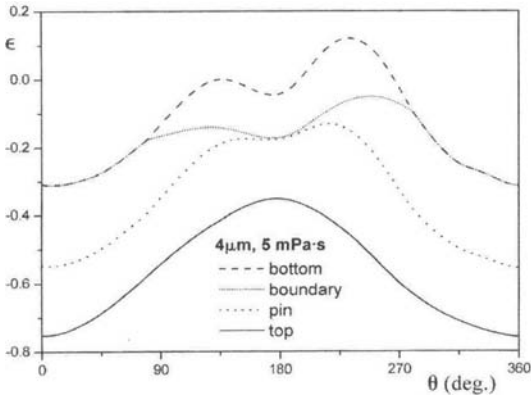
Fig. 4 The x-direction orbits at 4 locations of the reciprocationg piston

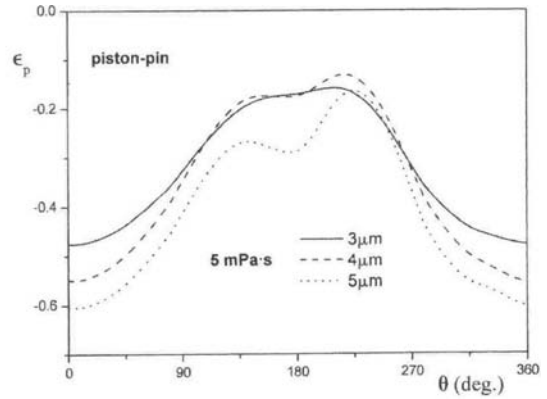**Fig. 5** Comparison of the piston-pin orbits variation in the radial clearance between piston and cylinder
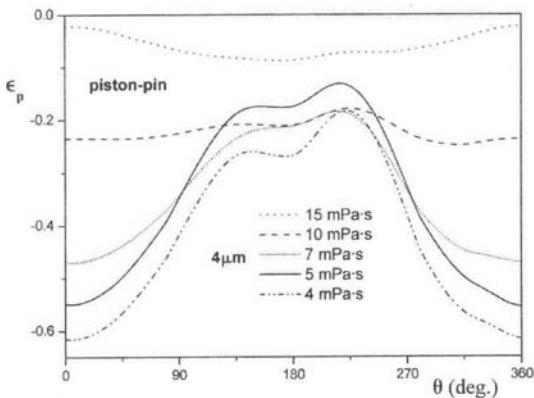

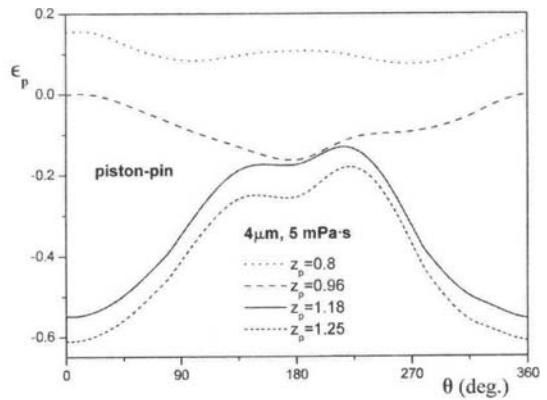**Fig. 6** Comparison of the piston-pin orbits variation in the lubricant viscosity

Fig. 7 Comparison of the piston-pin orbits variation in pin location of the piston

cylinder bore. The trajectory of the piston top center is closing on the thrust side of the cylinder wall, but the piston bottom center is lying on the center line of the cylinder. The influence of the radial clearance on the secondary oscillatory motion of the piston is presented in Fig. 5 for an entire cycle. From this figure, it is seen that small values of radial clearance results in increasing damping of the oil film which, in turn, tend to stabilize the secondary motion of the piston. The effect of the oil viscosity on the radial trajectory of the piston is shown in Fig. 6. From this result, it can be seen that the secondary trajectory increases with decreasing oil viscosity. The influence of the wrist-pin location on the lateral behaviour of the piston within the cylinder is

shown in Fig. 7. From this figure, it is seen that stability of the piston increases with decreasing the value of piston pin location. At the value of $z_p = 0.8$, the wrist-pin is located at the mid point between top and bottom of the piston. It can be shown that as the wrist-pin location approaches to the mid point of the piston, the trajectory of the piston can be stabilized. The effect of the length of cylinder wall on the piston trajectory is shown in Fig. 8. The stability of piston increases with increasing the length of cylinder up to a certain value and then tends to approach to a concave type trajectory closing to the anti-thrust side of the cylinder wall. As seen in Fig. 9, the averaged power consumption per cycle for the fixed value of clearance of 4 increases almost linearly with

Table 2 Friction loss, oil leakage, and minimum oil film thickness on various values of the oil viscosity and the radial clearance

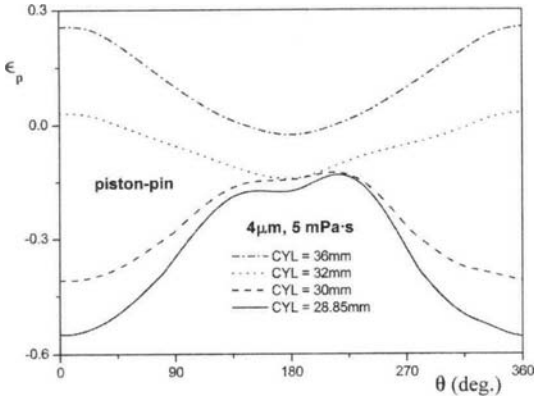| Parameters — Viscosity (mPa·s)	Classification — Clearance (μm)	Power consumption (W)	Oil leakage (cm³/h)	Minimum oil film thickness (μm)
	2	14.115	8.460	1.661
	3	10.414	3.412	2.063
	4	8.393	8.701	2.739
	5	7.744	17.571	3.145
4		7.768	11.372	2.479
5		8.393	8.701	2.739
7	4	10.948	5.713	2.710
10		14.286	3.440	3.123
15		20.764	2.091	3.505

Fig. 8 Comparison of the piston-pin orbits variation in the length of cylinder
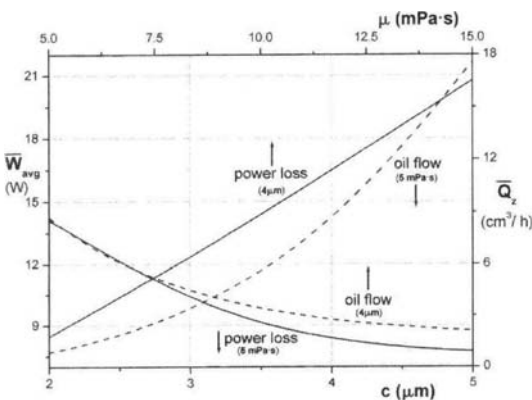

Fig. 9 Cycle averaged power consumption and oil leakage as a function of the radial clearance and the lubricant viscosity

the oil viscosity. In the same condition, the variation of the averaged oil leakage per cycle with lubricant viscosity parameter is shown. And, the averaged power consumption per cycle for the fixed value of viscosity 5 mPa·s is shown with the various values of the side clearance of piston. Also, the averaged oil leakage per cycle as a function of clearance of the piston is shown in the same figure. The friction loss, oil leakage, and minimum oil film thickness for various values of the oil viscosity and side clearance are summarized in Table 2. From these results, the friction loss and minimum film thickness between piston and cylinder wall increases with increasing oil viscosity, but oil leakage decreases with increasing viscosity. And, enlarging the clearance between piston and cylinder, oil leakage and minimum film thickness increase, but power consumption decreases.

4. Conclusions

A mathematical model was developed for the secondary dynamic analysis of reciprocating pistons. The analysis incorporated the dynamic equation for piston as well as the hydrodynamic lubrication equation applied to the oil film between piston and cylinder. A computer program developed on this model can be used to analyze the secondary dynamic characteristics of recipro-

cating piston by calculating the trajectory of the piston, power consumption and oil leakage. The influence of the radial clearance, oil viscosity, pin location, and length of cylinder wall on the piston dynamics and lubrication characteristics are examined. Among the results, it was shown that stable piston trajectory can be obtained if the wrist-pin location is approached to the mid point of the piston. It was also found that the piston stability can be significantly improved by modifying the length of cylinder to the optimum condition. The program presented can be used as helpful tool in assessing the influence of design parameters on the stability of piston trajectory and characteristics of hydrodynamic lubrication.

Acknowledgment

References

Cho, S. H., Ahn, S. T. and Kim, Y. H., 2000, "A Model of Collision Point to Estimate Impact Force Related to Piston Slap," *Journal of KSNVE*, Vol. 10, No. 3, pp. 474~479. (In-Korean)

Etsion, I. and Gommed, K., 1995, "Improved Design with Non-cylindrical Profile of Gas Lubricated Ringless Piston," *Trans ASME, Journal of Tribology*, Vol. 117, pp. 143~147.

Gommed, K. and Etsion, I., 1993, "Dynamic Analysis of Gas Lubricated Reciprocating Ringless Piston-Basic Modeling," *Trans ASME, Journal of Tribology*, Vol. 115, pp. 207~213.

Gommed, K. and Etsion, I., 1994, "Parametric Study of the Dynamic Performance of Gas Lubricated Ring-less Piston," *Trans ASME, Journal of Tribology*, Vol. 116, pp. 63~69.

Kim, T. J., 2001, "Dynamic Behavior Analysis of a Crankshaft-Bearing System in Variable Speed Reciprocating Compressor," *Journal of KSTLE*, Vol. 17, No. 6, pp. 426~434. (In-Korean)

Li, D. F., Rohde, S. M. and Ezzat, H. A., 1983, "An Automotive Piston Lubrication Model," *ASLE Transactions*, Vol. 26, No. 2, pp. 151~160.

Nakada, T., Yamamoto, A. and Abe, T., 1997, "A Numerical Approach for Piston Secondary Motion Analysis and its Application to the Piston Related Noise," SAE paper No. 972043.

Prata, A. T., Fernando Julio R. S. and Fagotti, F., 2000, "Dynamic Analysis of Piston Secondary Motion for Small Reciprocating Compressor," *Trans ASME, Journal of Tribology*, Vol. 122, pp. 752~760.

Zhu, D., Cheng, H. S., Arai, T. and Hamai, K., 1992, "A Numerical Analysis for Piston Skirts in Mixed Lubrication Part 1 : Basic Modeling," *Journal of Tribology*, Vol. 114, pp. 553~562.

Zhu, D., Hu, Y. Z., Cheng, H. S., Arai, T. and Hamai, K., 1993, "A Numerical Analysis for Piston Skirts in Mixed Lubrication Part 2: Deformation Consideration," *Journal of Tribology*, Vol. 115, pp. 125~133.